ACS APPLIED MATERIALS & INTERFACES

Research Article

www.acsami.org

Oriented Clay Nanopaper from Biobased Components—Mechanisms for Superior Fire Protection Properties

F. Carosio,*[,†,‡] J. Kochumalayil,[†] F. Cuttica,[‡] G. Camino,[‡] and L. Berglund[†]

[†]Department of Fiber and Polymer Technology, Wallenberg Wood Science Center, Royal Institute of Technology, SE-10044 Stockholm, Sweden

[‡]Politecnico di Torino, Alessandria Site, Viale Teresa Michel 5, 15121 Alessandria, Italy

Supporting Information

ABSTRACT: The toxicity of the most efficient fire retardant additives is a major problem for polymeric materials. Cellulose nanofiber (CNF)/clay nanocomposites, with unique brick-and-mortar structure and prepared by simple filtration, are characterized from the morphological point of view by scanning electron microscopy and X-ray diffraction. These nanocomposites have superior fire protection properties to other clay nanocomposites and fiber composites. The corresponding mechanisms are evaluated in terms of flammability (reaction to a flame) and cone calorimetry (exposure to heat flux). These two tests provide a wide spectrum characterization of fire protection properties in CNF/montmorrilonite (MTM) materials. The morphology of the collected residues after flammability testing is investigated. In addition, thermal and thermo-oxidative stability are evaluated by thermogravimetric analyses performed in inert (nitrogen) and oxidative (air) atmospheres. Physical and chemical mechanisms are identified and related to the unique nanostructure and its low thermal conductivity, high gas barrier properties and CNF/MTM interactions for char formation.

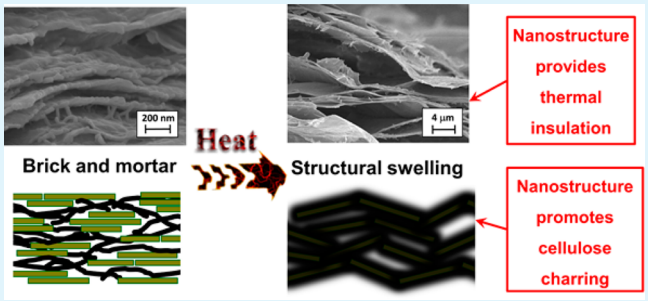

KEYWORDS: *nanocellulose, nanocomposite, biocomposite, layered silicate, brick and mortar, thermal stability, fire protection*

INTRODUCTION

Flame retardants are widely used additives in plastics and composites. Recently, the safety and efficiency of flame retardants have been questioned.[1] The flame retardant chemicals do not always function as well as expected and may pose toxic hazards. As an example, halogenated compounds have been found in the food chain and in the bodies of animals and humans.[2] For these reasons, nontoxic fire retardants are of industrial and scientific interest. Furthermore, introduction of biobased components as fire retardants would meet societal demands of increased use of green, sustainable materials. In previous studies, polymer nanocomposites have demonstrated remarkable improvements in mechanical strength, oxygen barrier properties and flammability.[3−5] The results are typically achieved with low amounts of inorganic nanoparticle (usually below 5 wt %). An important reason is that nanostructural control is problematic during melt-processing or thermoset molding of composites. For instance, it is challenging to homogeneously dispersion nanoparticles in the polymer matrix.

Recently, nanocellulose in the form of nanofibrillated cellulose (CNF) has attracted interest as a plant-based building block for nanocomposites. CNF is conveniently disintegrated from wood fibers.[6] Typical dimensions are 3−15 nm in diameter and 0.7−3 μm in length. Swirled rather than straight CNF conformations are typical in nanopaper structures. Water-based CNF colloids can be filtered in paper-like processing to form nanostructured films,[7] with interesting mechanical and physical properties including optical transparency, gas barrier properties[8] and low thermal expansion. Nanocellulose has been classified into three main groups: cellulose nanocrystals (CNC), cellulose nanofibers (CNF) and bacterial nanocellulose (BNC).[9,10] CNC are rodlike particles obtained from cellulose subjected to acid hydrolysis and typically have a width of 3−10 nm and lengths in the 150 nm-1 μm range. BNC is generated by aerobic bacteria, rendering a ribbon width on the order of 50−100 nm. In the pellicle produced by the bacteria it is difficult to find ribbon ends. Among the different types of nanocellulose, wood-based CNF is particularly interesting since numerous pilot plants are in operation around the world. The CNF cost is expected to be much lower than for BNC or CNC. Because of the feasibility of filtration processing of CNF hydrocolloids, CNF also has potential in large-scale nanotechnology applications, where the manufacturing is carried out by modified paper-making approaches.

In previous work, CNF was mixed in colloidal suspension with montmorrilonite clay platelets (MTM) and filtered to

Received: December 23, 2014
Accepted: February 27, 2015
Published: February 27, 2015

DOI: 10.1021/am509058h
ACS Appl. Mater. Interfaces 2015, 7, 5847−5856

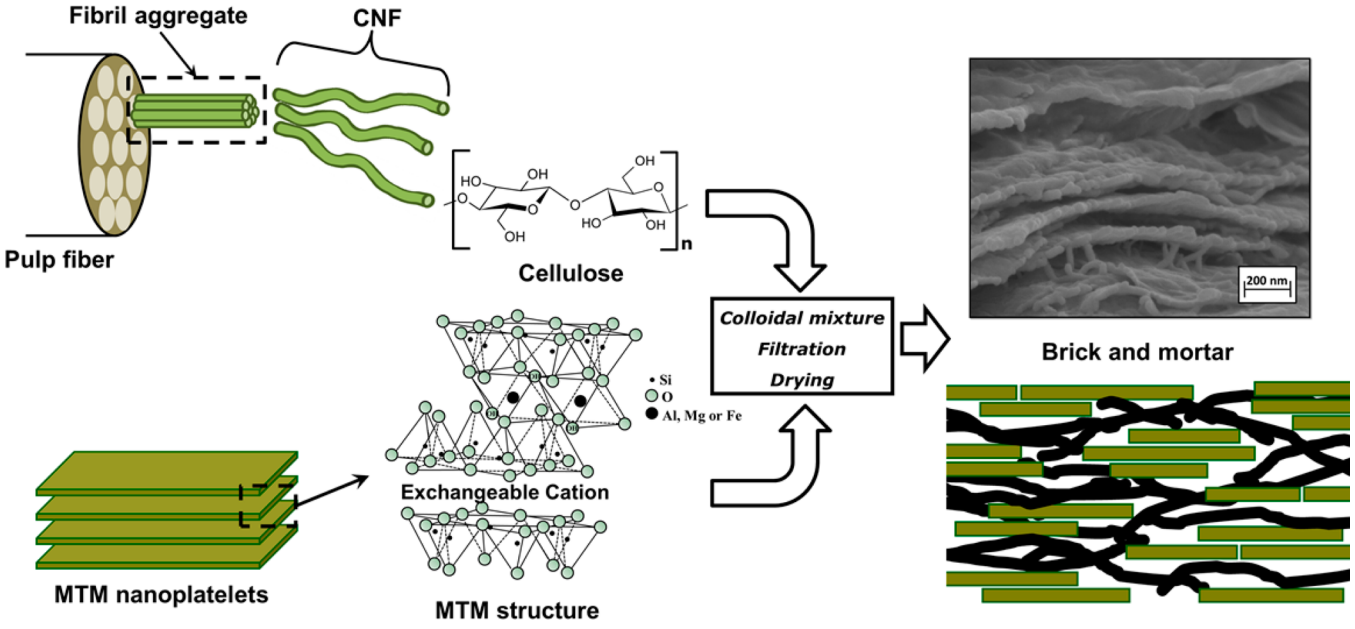

Figure 1. Schematic representation of the CNF/MTM nanopaper constituents and final structure.

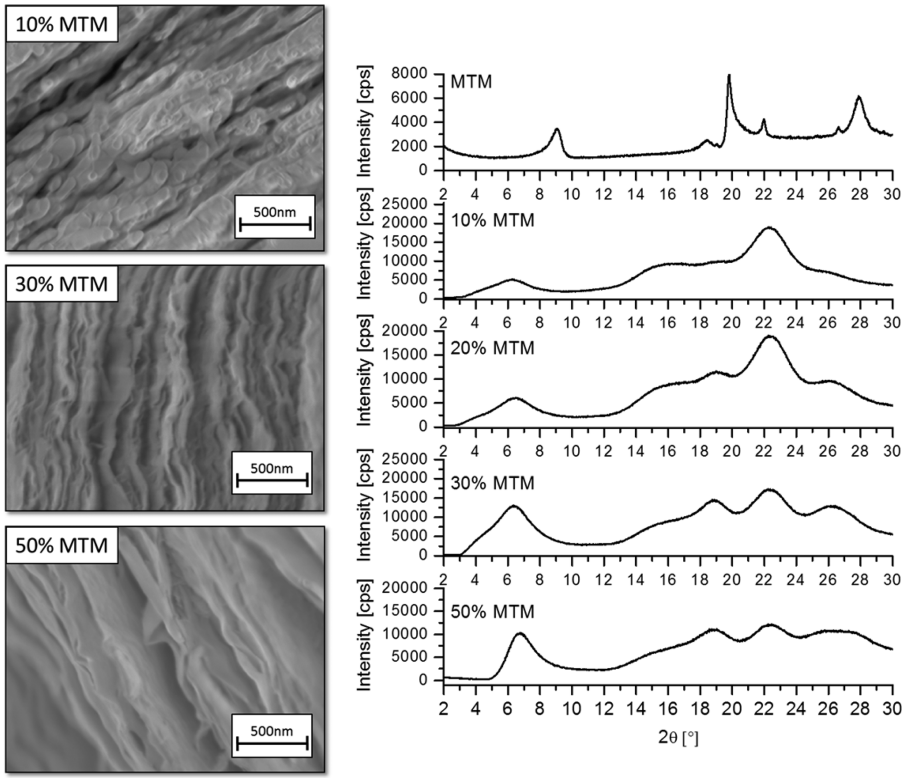

Figure 2. SEM micrographs of microtome cut cross sections and XRD spectra of CNF/MTM nanocomposites with weight fractions of MTM content according to the designations.

form "clay nanopaper" with strong in-plane orientation of MTM,[11] as described in Figure 1.

The CNF forms a nanofiber network, which serves as a continuous matrix around oriented MTM platelets and imparts toughness and strength. The papermaking approach was further improved to shorten filtration time.[12] Mechanical properties were improved by the use of oxidized CNF, which provides stronger CNF/MTM interaction.[13] The TEMPO-oxidized CNF tends to be difficult to filtrate though.

The high thermal and flame shielding characteristics displayed by CNF/MTM brick and mortar nanocomposites are of scientific and technical interest.[11] Although the use of clay either as a reinforcement particle for bulk composites, aerogels, or as a thin coating constituent has demonstrated interesting flame retardant features,[14−19] quantification of properties is still limited and corresponding mechanisms are not very clear. Furthermore, as reported in the literature for other MTM/polymer nacre-mimetics materials,[20,21] the nano-

DOI: 10.1021/am509058h
ACS Appl. Mater. Interfaces 2015, 7, 5847−5856

structured CNF/MTM brick and mortar biocomposites appear to provide unique fire retardant properties. Possible structural reasons include high clay content, oriented "bricks" and unique degradation mechanisms for CNF in the presence of MTM. Another argument, which makes this class of material interesting, is the green processing route and its potential for large scale and continuous production of comparably thick (100 μm) nanopaper films.[22] Such films may, in analogy with prepreg technologies, be laminated to form nanostructured engineering materials. They can also be used as loadbearing surface materials for fire protection of engineering structures, such as fiber composites used in train interior applications.

Rational development of nontoxic and nonflammable brick and mortar nanocomposites would be greatly facilitated if the mechanisms controlling flammability and degradation were known. Very few previous studies have even attempted to explain these fairly complex mechanisms. For this purpose, Grunlan and co-workers combined thermogravimetric analysis (TGA) with flammability testing of clay-coated fabrics.[17] Subsequently, they studied biocomposite clay/polymer coatings of high inorganic content prepared by LbL, for the purpose of foam protection.[18] The improved methodology included cone calorimetry in order to better understand flammability data.

In the present paper, the first study of flame shielding mechanisms in brick and mortar type of clay biocomposite films (high content of clay with high in-plane orientation) is reported. These materials extend the potential applications for thin clay-containing LbL-films and coatings so that bulk materials and larger thickness films can be manufactured. The study has particular focus on nanocellulose since this component forms tough networks, is widely available at low cost, is from renewable resources and appear to show unique flame shielding characteristics. The objective is to quantify flame retardancy properties of CNF/MTM, elucidate the operating mechanisms for flame retardancy and initiate development of materials design principles for green and nonflammable CNF/MTM biocomposites. MTM clay content is varied (from 10 to 50 wt %). In short, the main flame retardancy mechanisms are identified, several material compositions are found to be nonflammable, and the study makes it possible to more systematically design new flame-retardant nanomaterial systems. Finally, a proof of concept is presented for the application of clay nanopaper as thin protective surface layers for composites. Uncoated and coated composite demonstrators are subjected to cone calorimetry tests mimicking exposure to a developing fire.

RESULTS AND DISCUSSION

CNF nanofibers in colloidal suspension were mixed with the supernatant fraction of unmodified MTM platelets in suspension. This reduces the risk for formation of major agglomerate structures in the material. The mixture was filtered and dried to form clay nanopaper films according to the description in the Experimental Section.

Morphology. SEM microscopy was combined with X-ray diffraction (XRD) to assess the morphology of the CNF/MTM nanocomposites. Figure 2 reports micrographs and XRD spectra of CNF/MTM nanocomposites with 10, 30, and 50% by weight of MTM (10% MTM, 30% MTM, 50% MTM).

CNF/MTM nanocomposites show ordered nanostructures in which MTM nanoplatelets oriented in the plane and tactoids are intercalated by CNF. As MTM content is increased from 10% to 50%, the individual nanoplatelets and their morphology at larger scale become more visible. The in-plane orientation is apparent, in particular at the 30% MTM content, whereas 50% MTM sample shows a reduced orientation probably due to sample cutting process performed prior to SEM observations. The XRD measurements provide additional information. Neat MTM shows the characteristic peak at 9.0° (9.7 Å) characteristic of the basal spacing between each MTM nanoplatelet, which is consistent with the literature.[23,24] In nanocomposites, a peak is observed to be centered around 6.0°. This indicates that the average MTM interlayer distance has been increased to higher values (13.4 Å) because of hydration effects. This peak is observed in all compositions, but increases in intensity with increased MTM content. For 30% MTM and 50% MTM samples, intensity values are twice those of neat MTM. This is due to the ordered brick and mortar structure with nanoplatelets parallel to each other. The peak then shows greater diffraction intensity compared with neat MTM powder with random nanoplatelet orientation in space.

Thermal and Thermo-oxidative Stability. The thermal and thermo-oxidative stability of neat CNF and CNF/MTM nanocomposites was assessed by thermogravimetric analyses in nitrogen and air, respectively. The purpose is to obtain more basic degradation information, useful for further interpretation of cone calorimetry and flammability data. Figure 3 reports TG and dTG curves in nitrogen of CNF and for the clay containing nanocomposites; Table 1 reports TGA data obtained from the plots.

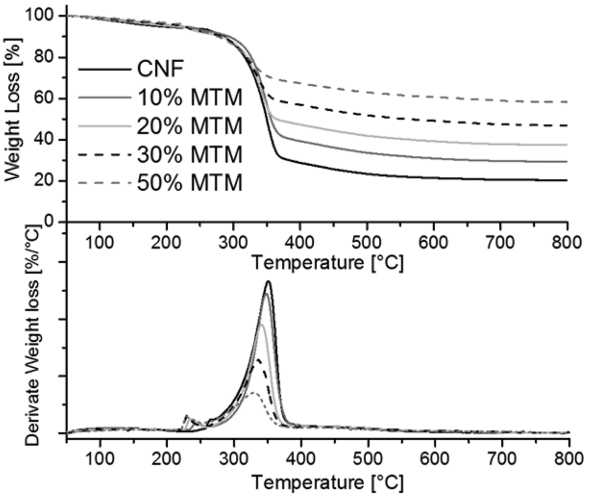

Figure 3. TG and dTG plots of CNF and CNF/MTM nanocomposites in nitrogen.

First, thermal degradation of CNF cellulose is evaluated for the nitrogen environment (no oxidation). The loss of the first 6 wt % can be ascribed to the removal of moisture. Neat CNF shows thermal degradation similar to pure cellulose, with one step of weight loss (300−400 °C) resulting from two competitive pathways. The first one is depolymerization of the glycosyl units to volatile products (levoglucosan). The second one, in competition with the first one, is decomposition of the same units to thermally stable aromatic char, which forms the final residue collected at the end of the test (20%).[25]

When CNF is combined with MTM at different concentrations, no significant change occurs in cellulose degradation, it still proceeds in one step. The 10 wt % MTM nanocomposite shows a slight increase in T_{onset}; however, at higher clay

DOI: 10.1021/am509058h
ACS Appl. Mater. Interfaces 2015, 7, 5847−5856

Table 1. Thermogravimetric Data of CNF and CNF/MTM Nanocomposites in Nitrogen[a]

Sample	$T_{onset10\%}$ [°C]	T_{max}* [°C]	Tot. residue at 800 °C [%]	Organic residue** at 800 °C [%]
CNF	285	350	20	20
10% MTM	293	347	31	23
20% MTM	281	339	39	24
30% MTM	280	335	49	27
50% MTM	278	327	60	21

*From derivative TG curves. **% of residue attributed to the organic CNF, calculated as reported in the experimental section [a]The reported residue is in wt% of total CNF content.

contents a slight decrease is observed for T_{onset}, as reported in Table 1. The degradation rate of CNF in CNF/MTM nanocomposites appears to be reduced compared with pure CNF. Indeed, the peak height corresponding to maximum weight loss rate is reduced with increased clay content, see dTG curves reported in Figure 3. This effect is ascribed to the brick and mortar structure, in particular the oriented clay nanoplatelet "bricks". MTM organized in this specific manner functions as a thermal insulation shield, which reduces heat transfer rate and thus reduces the degradation rate.[26] Furthermore, the total organic residue at 800 °C increases proportionally with clay content, see Table 1 and Figure 3. If the amount of water lost in the 100−200 °C range is taken into account, it is observed that all nanocomposites showed increased CNF residue compared with neat CNF, see Table 1. The MTM nanoplatelets apparently increase the char production of CNF, partly by acting as a thermal insulator. MTM probably also is a catalyst for char-producing degradation of CNF, due to the presence of Na^+ ions on the clay surface. Indeed, metal ions are capable of enhancing the char production of cellulose when present in catalytic concentrations.[27,28] It is worth mentioning that the increased char yield is strongly related to the present nanostructure with intimate contact between high specific surface clay and CNF.

The thermo-oxidative stability was also evaluated by TG analyses performed in air; Figure 4 reports TG and dTG plots while Table 2 collects data calculated from TGA plots.

As can be observed from Figure 4, the thermal oxidation of neat CNF takes place in two steps. The first occurs in the range between 300 and 400 °C and is due to formation of both volatiles and aliphatic char; this latter char is further oxidized during the second degradation step between 400 and 600 °C with the production of both CO and CO_2.[29]

Surprisingly, for the CNF/clay nanocomposites, only one degradation step is observed in the 300−400 °C range. The expected second degradation step with oxidation of neat CNF is almost completely suppressed. No peak can be detected in the dTG curves of CNF/clay compositions. This does not mean that there is no weight loss, since there is a considerable difference in the amount of residue produced at 400 and 800 °C, respectively, see Table 2. After the first degradation step, the char is only partially oxidized. Then continued oxidative degradation takes place at a slow rate. As already observed in nitrogen, all CNF/clay compositions showed a final content of residues higher than the starting inorganic content. The content of residues is slightly lower than for the nitrogen case, as

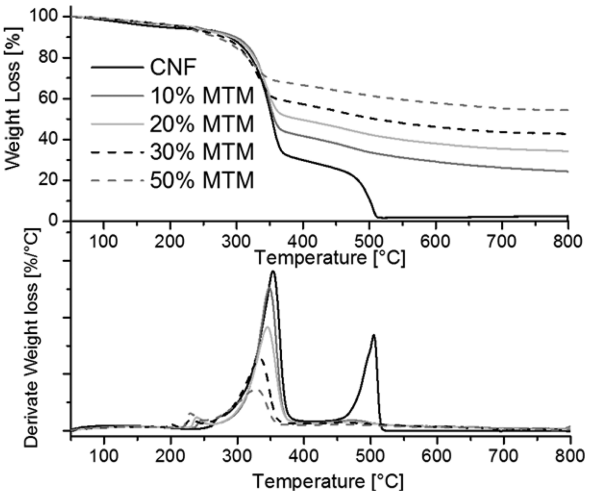

Figure 4. TG and dTG plots of CNF and CNF/clay nanocomposites in air.

Table 2. Thermogravimetric Data of CNF and CNF/MTM Nanocomposites in Air[a]

sample	$T_{onset10\%}$ [°C]	T_{max1} [b] [°C]	T_{max2} [b] [°C]	residue at 400 °C [%]	residue at 800 °C [%]	organic residue[c] at 800 °C [%]
CNF	289	353	505	30	<2.0	<2.0
10% MTM	298	348	NA	41	25	17
20% MTM	293	346	NA	50	36	19
30% MTM	280	334	NA	58	45	21
50% MTM	269	328	NA	67	57	13

[a]The reported CNF residue is in wt % of total CNF content. Residue is in wt % of total CNF/MTM mass. [b]From derivative TG curves. [c]% of residue attributed to the organic CNF, calculated as reported in the Experimental Section

expected. In contrast to the neat CNF, a substantial fraction of CNF char survives to 800 °C because of the ordered nanostructure of the CNF/clay nanocomposites. The thermal barrier exerted by clay and the catalytic effect of the Na^+-rich MTM surface promotes char formation and slows down the degradation of this residue in the second step. However, the second degradation step of CNF is mainly because of oxidation, and for this reason the oxygen barrier properties of the present material are also important. The CNF/clay nanostructure creates a tortuous path, which greatly reduces oxygen diffusion due to the preferential orientation of clay lamellae parallel to the film surface and this maximizes the barrier effect.[12] All three mechanisms listed above contribute to the final residue, possibly with some degree of interaction: the reduced heat transfer and oxygen diffusion enhances CNF char formation catalyzed by the MTM surface, which is rich in sodium ions.

Flammability. To assess the potential of CNF/clay nanocomposites in fire protection, it is necessary to test the response to a direct flame (flammability test). This evaluates the propensity of the material to initiate fire and is used for evaluation of fire protection properties of polymer composites and nanocomposites.[30] Vertical flammability tests were performed; Table 3 reports observations during the test, while Figure 5 contains snapshots of the residues collected after the test.

DOI: 10.1021/am509058h
ACS Appl. Mater. Interfaces 2015, 7, 5847−5856

Table 3. Flammability Data from Vertical Flammability Test of CNF and CNF/MTM Nanocomposites[a]

sample	total burning time [s]	afterglow time [s]	residue [%]
CNF	9	15	0
10% MTM	8		25
20% MTM	16		55
30% MTM	5		76
50% MTM	2		95

[a]Residue is in wt % of total mass.

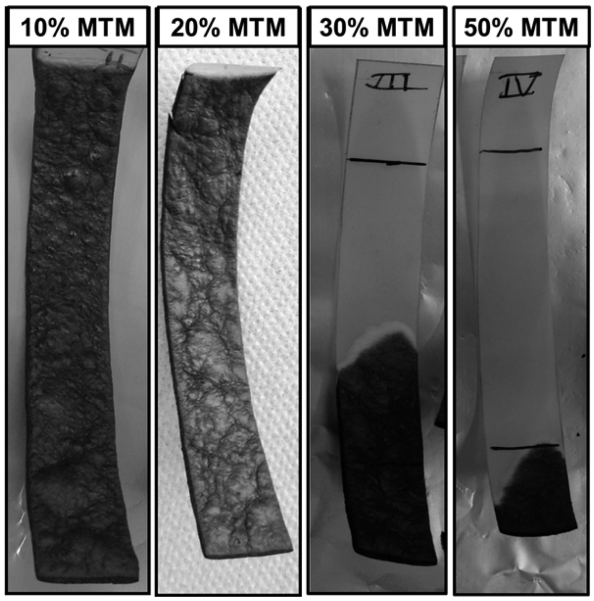

Figure 5. Residues collected after vertical flammability test of CNF/Clay nanocomposites. The fraction of original mass retained is reported as residue in Table 3

Upon methane flame application, neat CNF ignites immediately and burns with vigorous flames. The flames spread rapidly to the entire length of the sample. After on average 9 s, the flame is extinguished and an afterglow phenomenon is observed. This is flameless combustion (red glowing) and it completely consumes the remaining CNF residue. Although the flame is not present, flameless combustion can still be a safety threat. For instance, the high temperatures during afterglow can spread the fire to other ignitable and flammable materials.

CNF/clay nanocomposites show differences in behavior for different clay contents. 10% MTM and 20% MTM samples burn completely, although a coherent charred residue remains, see Table 3. The charred remains have the same dimensions as the starting sample, but with increased thickness (Figure 5). None of these two CNF/MTM compositions showed any afterglow phenomenon. The 20% MTM samples showed increased burning time (+77% compared with pure CNF) since the presence of clay reduced the speed of flame spreading.

As the clay content was increased to 30% or above, a threshold in flammability was observed. Both the 30% and 50% MTM samples showed self-extinguishing behavior. After ignition by the methane flame, the advancing flame is gradually reduced in size and rate of spreading as it becomes located in a progressively smaller section of the sample, where the flame eventually vanishes. Furthermore, any subsequent application of the methane flame could not reignite the sample. This behavior is important since a potential fire threat can be suppressed by self-extinguishing behavior. Also, the amount of residues left after combustion is extremely high as reported in Table 3.

The formation of ordered MTM nanoplatelets in the CNF nanofiber network matrix resulted in strongly improved flammability behavior. The properties were enhanced with increased inorganic content. The visually observable mechanisms during exposure to the flame are basically the same, regardless of clay content, although the final behavior and final result are different.

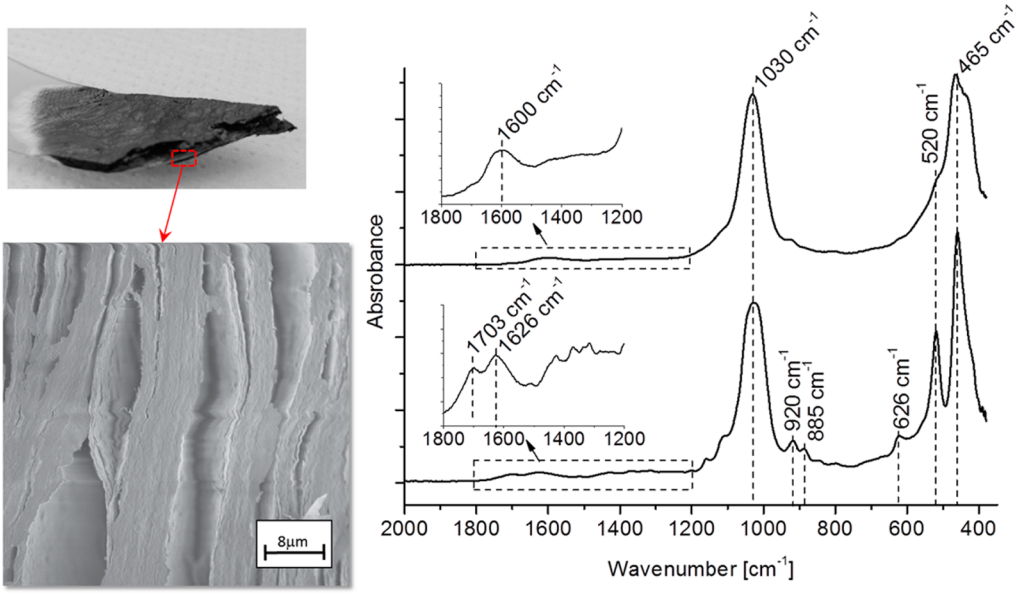

Figure 6. Images from a cross-section of CNF/30%MTM nanocomposite residue collected after vertical flame test (left part of composite figure) and ATR spectra of absorbance versus wavenumber measured on the surface of the residue (upper ATR diagram) and measured at the center of the cross section (lowest ATR diagram).

DOI: 10.1021/am509058h
ACS Appl. Mater. Interfaces 2015, 7, 5847−5856

Analysis of Char Residue and Microscale Porosity. The residue collected after flammability tests was investigated in order to assess the changes in morphology and composition imparted by the flame. Figure 6 reports an image of a CNF/30%MTM nanocomposite residue. The SEM micrograph is from the cross-section of a region subjected to partial combustion and the ATR spectra were obtained at different distances from the sample surface.

SEM micrographs of the cross section of the burned region (residue) reveal the morphology after the test. The most interesting feature is that the CNF/30%MTM structure contains microscale voids. The voids are responsible for the overall macroscopic thickness expansion in the samples from vertical flame and cone calorimetry tests. Voids are formed because of the release of volatile degradation products from CNF so that the structure is expanded in thickness direction. ATR spectroscopy of regions in the cross-sectional plane reveals differences in residue composition with distance from the surface. Data collected from the surface are dominated by signals from the inorganic MTM (stretching Si−O−Si at 1030 cm^{-1}, bending Si−O−Si at 465 cm^{-1}).[31] The CNF appears to be completely degraded with virtually no residues. In contrast, spectra collected from the center of the sample (Figure 5, bottom right) show new peaks ascribed to condensed charred structures from the pyrolysis of CNF. The structures are aromatic since a double bond peak is found at 1626 cm^{-1} and two more peaks related to char are observed at 920 and 885 cm^{-1}. However, there are also carboxyl groups at 1703 cm^{-1} and the expected triplets for charred structures in the 900−700 cm^{-1} region are absent. This suggests the aromatic structures have different degrees of substitution and can be considered as precursors of fully aromatic char.[32]

EDS analyses performed on different regions of the residue cross section confirmed the higher organic content at the center compared with the surface, Supporting Information Figure S2.

Cone Calorimetry. Cone calorimetry was employed to assess the resistance of the materials to the exposure of an heat flux typical of a developing fire scenario. Although this method can be used to evaluate the heat flow kinetics during flame development, the present purpose was to evaluate the potential for nonflammable behavior. This is an unusual but highly desirable characteristic of polymeric materials. Neat CNF and CNF/MTM samples were exposed to a heat flux of 35 kW/m^2. This heat flux represents the early stage of a developing fire, and the objective is to assess the sensitivity to ignition (as a consequence of the heat flux). The collected information is reported in Supporting Information Table 1S. During cone calorimetry, the sample is subjected to constant heat flux. A spark is generated continuously, so that under certain conditions the material will ignite and be subjected to combustion. As far as neat CNF is concerned, upon exposure to the heat flux the temperature is increased and, according to the previous TGA data (Figures 3 and 4), CNF degrades and releases volatile gases. When the concentration of ignitable volatiles is sufficient, ignition takes place and the sample is subjected to virtually complete combustion through oxidation. No residue is found at the end of the CNF test as reported in Supporting Information Table S1 and Figure S3.

CNF/clay nanocomposites showed much enhanced fire protection properties compared with neat CNF. Surprisingly, 30% MTM and 50% MTM nanocomposites did not ignite at all during cone calorimetry tests. This result is extremely unusual for polymer materials. As the CNF/30% MTM and CNF/50% MTM brick and mortar compositions are exposed to the heat flux, the volatile gases released as a result of CNF degradation do not reach the concentration required for ignition. All nanocomposite samples produced a coherent residue and showed increased sample thickness, as observed after vertical flame tests. The absolute amount of residue increased with clay content, and the final value is higher than the amount of initial inorganic phase. A fraction of organic degradation products from CNF is apparently present at the end of the test. It is worth mentioning that tests where ignition occurred lasted about 80 s, whereas nonigniting samples were tested for as long as 180 s to verify that the specimens could not be ignited.

From flammability and cone calorimetry data, the MTM concentration representing substantial changes in the fire protection behavior is 30% by weight. The tensile strength is around 80 MPa with a modulus of 7 GPa.[11] The CNF/30% MTM clay nanopaper surface layer (100 μm thickness) was used as a materials concept for fire protection of glass fiber/epoxy (GF/EP) composites tested by cone calorimetry. Table 4 presents cone calorimetry data, and Figure 7 reports the average heat release rate and smoke production rate for uncoated and clay nanopaper coated composites.

Table 4. Time to Ignition (TTI), Peak of Heat Release Rate (pkHRR), and Total Heat Release (THR) Values Collected by Cone Calorimetry for Unmodified and CNF/30% MTM Coated Composite

sample	TTI [s]	pKHRR [kW/m^2]	THR [MJ/m^2]
composite	68 ± 4	285 ± 25	62 ± 7
CNF/30% MTM surface	299 ± 43	235 ± 8	47 ± 4

The average time to ignition (TTI) for the unmodified GF/EP composite was 68 s. Then the composite started burning, and dark and dense smoke was released. The average heat release rate peak (pkHRR) was 285 kW/m^2. The use of the protective clay nanopaper on the GF/EP composite surface results in a significant increase in TTI that shifts from 68 to 299 s for the unmodified and coated composite, respectively (Figure 7). From a fire safety point of view, there is more time (4 min) to escape before ignition occurs. The pkHRR and THR values are reduced by 18% and 24%, with respect to the unmodified composite. Moreover, the delay in smoke production rate (Figure 7, SPR plots) indicates that no dense smoke is released prior to ignition. This is crucial since people confronted with smoke and its effects during evacuation[33] suffer from lost ability to react, unconsciousness, slower walking speed and long-term damages like neuropathology, sensitization and reactive airways disease syndrome.[34,35] Smoke-related effects makes smoke an important cause of fire fatalities.

Mechanisms for Nonflammable Properties. The previous sections have provided information on nanostructural brick and mortar organization, thermal degradation mechanisms, flammability data, and fire ignition response. Let us consider the CNF/30% MTM brick and mortar nanocomposite where the MTM platelets are well oriented parallel to the material surface and perpendicular to the direction of the heat flux (35 kW/m^2). On the basis of experiments and simulations, this structural polymer/clay configuration was recently reported to have among the lowest reported through-thickness thermal conductivity for any solid material.[26] This in combination with high heat capacity per volume and lack of degradation results in

DOI: 10.1021/am509058h
ACS Appl. Mater. Interfaces 2015, 7, 5847−5856

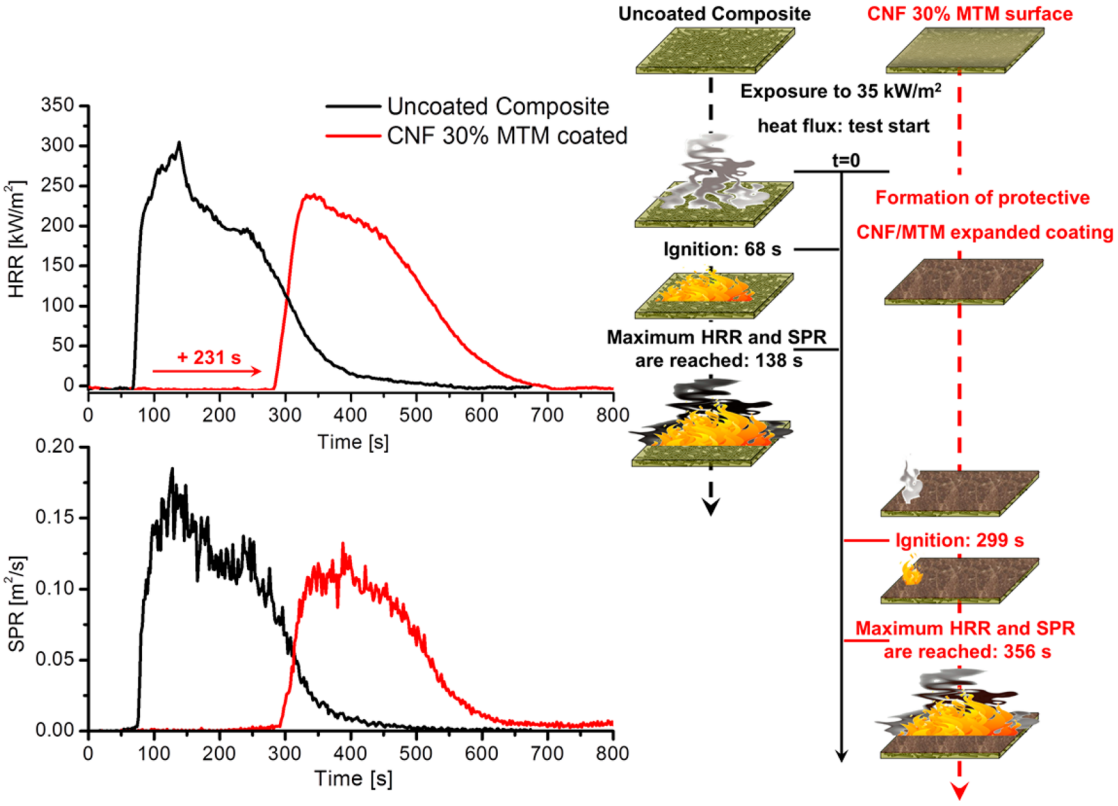

Figure 7. Heat release rate (HRR) and smoke production rate (SPR) plots of uncoated and clay nanopaper (CNF/30% MTM) coated GF/EP composites.

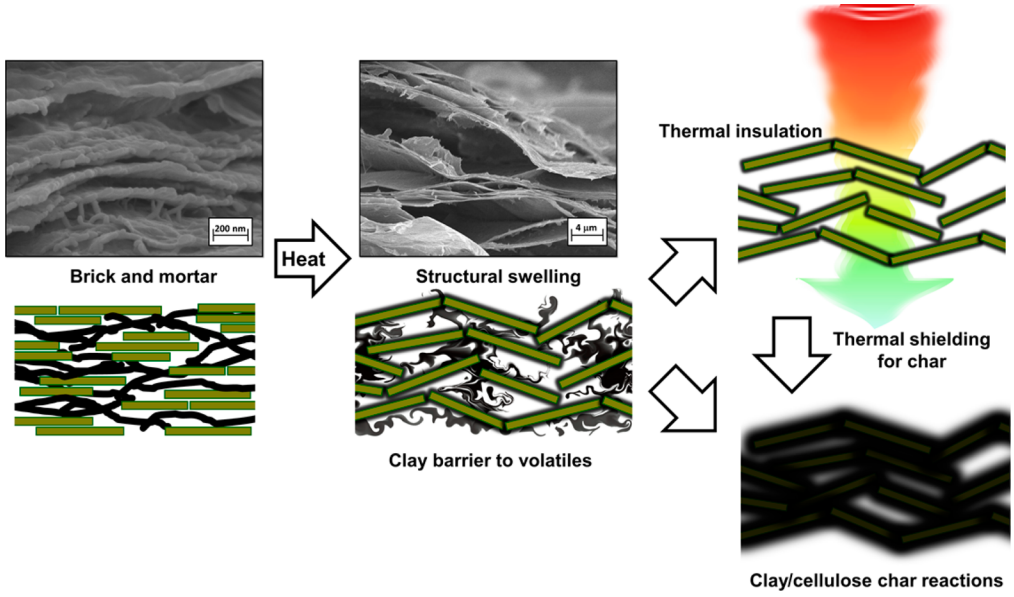

Figure 8. Schematic sketch of the fire proofing mechanism attributed to the CNF/MTM nanocomposites.

strong thermal shielding effects from the oriented clay constituent. Then the polymer phase needs to be considered. Compared with any polymer, the extended chain crystallite structure of nanofibrous cellulose results in highly favorable thermal degradation behavior that can be exploited for the preparation of carbon fibers because of the formation of thermally stable ladder polymers during carbonization.[36] The presence of oriented clay influences cellulose degradation in several ways. Thermal shielding leads to slow increase in local temperature. The oxygen barrier properties of oriented MTM, results in a locally oxygen-depleted environment. The presence of the Na^+-rich MTM surface next to the cellulose may catalyze favorable charring reactions.[27,28] As a consequence, a thermally fairly stable char is formed. Furthermore, the clay barrier hinders combustible volatiles produced from cellulose resulting in local void formation at the microscale, so that the thermal conductivity is further reduced. In conventional clay nanocomposites with low clay content, the surface will also be

DOI: 10.1021/am509058h
ACS Appl. Mater. Interfaces 2015, 7, 5847−5856

enriched in clay during combustion and facilitate charring of the polymer matrix.[37,38] However, the present brick and mortar structure is much better in terms of fire retardant properties because of the higher clay content, favorable clay orientation, better gas barrier and volatile hindering effects and large interfacial area. A sketch of the proposed fire proof mechanisms is presented in Figure 8.

CONCLUSIONS

The fire protection properties and their mechanisms in green and nontoxic cellulose-based clay nanocomposites have been thoroughly quantified and described based on flammability and cone calorimetry tests. The effects of different clay concentration have also been evaluated. The nanocomposite composition with 30 wt % montmorillonite shows self-extinguishing behavior during flammability tests. Furthermore, this brick and mortar nanocomposite with highly ordered clay platelets shows no ignition when exposed to heat fluxes typical of a developing fire scenario.

The main mechanisms can be summarized as follows: the in-plane orientation of the clay results in very low thermal conductivity so that CNF degradation is delayed. The barrier function of the clay then provides an oxygen-depleted environment during thermal degradation. Also, cellulose in its native highly ordered structure has a strong tendency to form thermally stable forms of char. This is further promoted by the proximity to the clay surfaces. As CNF volatiles are produced, the clay barrier hinders diffusion and ignition at the material surface. Instead, voids are formed so that thermal conductivity is further decreased. When employed as fire protective surface layers on GF/EP composites, the materials showed strongly increased time to ignition and delayed production of dangerous smoke. Nanocellulose-based oriented clay nanocomposites are thus proven to be a valuable, sustainable and efficient alternative to current flame retardant materials. The balance between fire retardant and mechanical properties is due to synergy between CNF and MTM clay for the specific nanostructure of clay nanopaper. Oriented MTM with numerous CNF/MTM interfaces provides barrier properties and low transverse thermal conductivity, whereas CNF provides toughness and favorable charring. Finally, the reported mechanisms make it possible to develop materials design principles for new organic/inorganic hybrids where fire retardancy and mechanical properties are optimized.

EXPERIMENTAL SECTION

Preparation of CNF/MTM Nanocomposites. The CNF was prepared from softwood sulfite pulp provided by Nordic Paper, Sweden in accordance with a previously reported method.[5] A 2 wt % pulp suspension was pretreated using an enzymatic degradation and mechanical beating prior to homogenization step. The resulting suspension was subsequently defibrillated by passing through a homogenization process using Microfluidizer M-110EH (Microfluidics Ind., USA) to form aqueous suspension of CNF. A 0.5 wt % montmorillonite (MTM) suspension (Cloisite Na^+, density of 2.86 g/cm^3, BYK Additives, Germany) was prepared by intense stirring using Ultra Turrax mixer (IKA, DI25 Basic) at 25000 rpm for 15 min followed by sonication using Vibra-Cell (Sonics & Materials, Inc.) for 5 min. The cycle was repeated three times and the final suspension was centrifuged at 4000 rpm for 20 min. The clay aggregates was discarded and the clear supernatant suspension was used for composite preparation. An aqueous composite suspension containing 5 g total solids was prepared by slowly adding the MTM suspension to a 1 wt % CNF suspension by mixing with Ultra Turrax at 12 000 rpm. The suspensions were kept for magnetic stirring overnight. The MTM concentrations in the composite suspensions were 10, 20, 30, and 50 (wt/wt %). The resulting suspensions were filtered through vacuum filtration set up using a wire net filter (325 × 2300 mesh) from Bopp Utildi AB, Sweden) following a procedure described elsewhere.[22] The films were dried under vacuum condition at 92 °C for 30 min achieving a final thickness of 100 μm.

Preparation of CNF/MTM Coated Glass Fiber Composites. Wet CNF-MTM films were hot pressed on glass fiber composite plates (100 × 100 × 3 mm, kindly provided by SICOMP in Piteå, Sweden) as schematically reported in Supporting Information Figure S1. The CNF/MTM dispersion was used as a glue to stick the sheets on the composite surface during vacuum hot-pressing (17.5 MPa and 140 °C for 30 min).

Characterization. *Field Emission-Scanning Electron Microscopy.* A high-resolution FE-SEM (Hitachi S-4800) was used for cross-sectional morphological analysis. The cross-sectional samples were prepared using a microtome blade cutting. The uncoated samples were analyzed in deceleration mode in SEM using a landing voltage of 0.3 kV. An electron current of 5 μA and a working distance of 1.5 mm were used.

X-ray Diffraction. X-ray diffraction (XRD) profile scans were recorded in reflection mode in the angular range of 0.5−30° (2θ). The measurements were performed with an X'Pert Pro diffractometer (model PW 3040/60). The CuKα radiation (1.5418 Å) generated with a tension of 45 kV and current 35 mA was monochromatized using a 20 μm Ni filter. A scan speed of 0.035°/ s and time per step of 60 s. were used. Samples were dried prior to experiment.

Thermal Stability. Thermogravimetric analyses (TGA) have been performed on a TAQ500 thermogravimetric balance from 50 to 800 °C (heating rate of 10 °C/min) in both nitrogen and air (60 mL/min). For each formulation, a square sample of 10 mg was placed in open alumina pans; the experimental error was 0.5% on the weight and 1 °C on the temperature. The final residue and CNF percentage in the final residue have been calculated taking into account the weight loss in the 50−150 °C range because of water removal.

Flammability. The flammability of prepared samples has been tested in vertical configuration; the sample (100 × 15 × 0.1 mm^3) was ignited from its short side by a 20 mm methane flame (flame application time: 5s). The test was repeated 3 times for each formulation to ensure reproducibility; during the test, parameters, such as burning time, afterglow times, and final residue, were registered.

Cone Calorimetry. Cone calorimetry (fire testing technology, FTT) was employed to investigate the combustion behavior of square samples (100 × 100 × 0.1 mm^3 CNF/MTM nanocomposites, 100 × 100 × 3 mm^3 epoxy composites) under 35 kW/m^2 in horizontal configuration, following the ISO 5660 standard. Because of sample excessive movements the tests have been performed adopting the edge frame and grid to maintain a constant distance between the sample and the conical heater. The test performed on uncoated and coated composite have been performed with the same configuration registering parameters, such as time to ignition (TTI, [s]), peak of heat release rate (pkHRR, [kW/m^2]), total heat release (THR, [MJ/m^2]), smoke production rate (SPR, [m^2/s]), and final residue were evaluated. For each formulation the test was repeated 3 times to ensure reproducibility

Fourier-Transformed Infrared Spectroscopy in Attenuated Total Reflectance. Attenuated total reflectance (ATR) Fourier transformed infrared spectroscopy spectra were collected at room temperature in the range 4000−400 cm^{-1} (32 scans and 4 cm^{-1} resolution) using a Frontier FT-IR/FIR spectroscopy (PerkinElmer, Italy) equipped with a diamond crystal (depth of penetration 1.66 μm, as stated by the producer).

ASSOCIATED CONTENT

Supporting Information

Description of the procedure adopted for the production of CNF/MTM coated glass fiber composites, EDS analyses performed on flammability residues, cone calorimetry data for

DOI: 10.1021/am509058h
ACS Appl. Mater. Interfaces 2015, 7, 5847−5856

CNF and CNF/MTM nanocomposites, and images of the residues collected after cone calorimetry tests. This material is available free of charge via the Internet at http://pubs.acs.org.

AUTHOR INFORMATION

Corresponding Author

* Federico Carosio, Tel.: +39 0131 229303, Fax: +39 0131 229399 E-mail: federico.carosio@polito.it.

Notes

The authors declare no competing financial interest.

ACKNOWLEDGMENTS

The authors would like to acknowledge the FireFoam project funded by SSF in Sweden.

REFERENCES

(1) Kemmleina, S.; Herzkeb, D.; Law, R. J. Brominated Flame Retardants in the European Chemicals Policy of REACH—Regulation and Determination in Materials. *J. Chromatogr. A* **2009**, *1216*, 320−333.

(2) Stieger, G.; Scheringer, M.; Ng, C. A.; Hungerbühler, K. Assessing the Persistence, Bioaccumulation Potential and Toxicity of Brominated Flame Retardants: Data Availability and Quality for 36 Alternative Brominated Flame Retardants. *Chemosphere* **2014**, *116*, 118−123.

(3) LeBaron, P. C.; Wang, Z.; Pinnavaia, T. J. Polymer-Layered Silicate Nanocomposites: An Overview. *Appl. Clay Sci.* **1999**, *15*, 11−29.

(4) Ray, S. S.; Okamoto, M. Polymer/Layered Silicate Nanocomposites: A Review from Preparation to Processing. *Prog. Polym. Sci.* **2003**, *28*, 1539−1641.

(5) Koo, J. *Polymer Nanocomposites: Processing, Characterization, and Applications*; McGraw-Hill Nanoscience and Technology: New York, 2006.

(6) Henriksson, M.; Henriksson, G.; Berglund, L. A.; Lindstrom, T. An Environmentally Friendly Method for Enzyme-Assisted Preparation of Microfibrillated Cellulose (MFC) Nanofibers. *Eur. Polym. J.* **2007**, *43*, 3434−3441.

(7) Henriksson, M.; Berglund, L. A.; Isaksson, P.; Lindstrom, T.; Nishino, T. Cellulose Nanopaper Structures of High Toughness. *Biomacromolecules.* **2008**, *9*, 1579−1585.

(8) Lavoine, N.; Desloges, I.; Dufresne, A.; Bras, J. Microfibrillated Cellulose—Its Barrier Properties and Applications in Cellulosic Materials: a Review. *Carbohydr. Polym.* **2012**, *90*, 735−764.

(9) Klemm, D.; Kramer, F.; Moritz, S.; Lindstrom, T.; Ankerfors, M.; Gray, D.; Dorris, A. Nanocelluloses: A New Family of Nature-Based Materials. *Angew. Chem., Int. Ed.* **2011**, *50*, 5438−5466.

(10) Sani, A.; Dahman, Y. Improvements in the Production of Bacterial Synthesized Biocellulose Nanofibres Using Different Culture Methods. *J. Chem. Technol. Biotechnol.* **2010**, *85*, 151−164.

(11) Liu, A.; Walther, A.; Ikkala, O.; Belova, L.; Berglund, L. A. Clay Nanopaper with Tough Cellulose Nanofiber Matrix for Fire Retardancy and Gas Barrier Functions. *Biomacromolecules.* **2011**, *12*, 633−641.

(12) Liu, A.; Berglund, L. A. Fire-retardant and Ductile Clay Nanopaper Biocomposites Based on Montmorrilonite in Matrix of Cellulose Nanofibers and Carboxymethyl Cellulose. *Eur. Polym. J.* **2013**, *49*, 940−949.

(13) Wu, C.; Saito, T.; Fujisawa, S.; Fukuzumi, H.; Isogai, A. Ultrastrong and High Gas-Barrier Nanocellulose/Clay-Layered Composites. *Biomacromolecules* **2012**, *13*, 1927−1932.

(14) Porter, D.; Metcalfe, E.; Thomas, M. J. K. Nanocomposite Fire Retardants—A Review. *Fire Mater.* **2000**, *24*, 45−52.

(15) Gilman, J. W.; Harris, R. H., Jr.; Shields, J. R.; Kashiwagi, T.; Morgan, A. B. A Study of the Flammability Reduction Mechanism of Polystyrene-Layered Silicate Nanocomposite: Layered Silicate Reinforced Carbonaceous Char. *Polym. Adv. Technol.* **2006**, *17*, 263−271.

(16) Carosio, F.; Alongi, J.; Frache, A. Influence of Surface Activation by Plasma and Nanoparticle Adsorption on the Morphology, Thermal Stability and Combustion Behavior of PET Fabrics. *Eur. Polym. J.* **2011**, *47*, 893−902.

(17) Li, Y.; Schulz, J.; Grunlan, J. C. Polyelectrolyte/Nanosilicate Thin-Film Assemblies: Influence of pH on Growth, Mechanical Behavior, and Flammability. *ACS Appl. Mater. Interfaces* **2009**, *1*, 2338−2347.

(18) Laufer, G.; Kirkland, C.; Cain, A.; Grunlan, J. C. Clay−Chitosan Nanobrick Walls: Completely Renewable Gas Barrier and Flame-Retardant Nanocoatings. *ACS Appl. Mater. Interfaces* **2012**, *4*, 1643−1649.

(19) Donius, A. E.; Liu, A. D.; Berglund, L. A.; Wegst, U. G. K. Superior Mechanical Performance of Highly Porous, Anisotropic Nanocellulose-Montmorillonite Aerogels Prepared by Freeze Casting. *J. Mech. Behav. Biomed. Mater.* **2014**, *37*, 88−99.

(20) Walther, A.; Bjurhager, I.; Malho, J.; Ruokolainen, J.; Berglund, L.; Ikkala, O. Supramolecular Control of Stiffness and Strength in Lightweight High-Performance Nacre-Mimetic Paper with Fire-Shielding Properties. *Angew. Chem., Int. Ed.* **2010**, *49*, 6448−6453.

(21) Das, P.; Schipmann, S.; Malho, J.; Zhu, B.; Klemradt, U.; Walther, A. Facile Access to Large-Scale, Self-Assembled, Nacre-Inspired, High-Performance Materials with Tunable Nanoscale Periodicities. *ACS Appl. Mater. Interfaces* **2013**, *5*, 3738−3747.

(22) Sehaqui, H.; Liu, A.; Zhou, Q.; Berglund, L. A. Fast Preparation Procedure for Large, Flat Cellulose and Cellulose/Inorganic Nanopaper Structures. *Biomacromolecules* **2010**, *11*, 2195−2198.

(23) Norrish, K. The Swelling of Montmorillonite. *Discuss. Faraday Soc.* **1954**, *18*, 120−134.

(24) Zheng, Y.; Zaoui, A. How Water and Counterions Diffuse into the Hydrated Montmorillonite. *Solid State Ionics.* **2011**, *203*, 80−85.

(25) Horrocks, A. R. In *Fire Retardant Materials*; Horrocks, A. R., Price, D., Eds.; Woodhead Publishing, Ltd.: Cambridge, England, 2001; Textiles, pp 128−181.

(26) Losego, M. D.; Blitz, I. P.; Vaia, R. A.; Cahill, D. G.; Braun, P. V. Ultralow Thermal Conductivity in Organoclay Nanolaminates Synthesized via Simple Self-Assembly. *Nano Lett.* **2013**, *13*, 2215−2219.

(27) Tian, C. M.; Guo, H. Z.; Zhang, H. Y.; Xu, J. Z.; Shi, J. R. Study on the Thermal Degradation of Cotton Cellulose Ammonium Phosphate and its Metal Complexes. *Thermochim. Acta* **1995**, *253*, 243−251.

(28) Soares, S.; Camino, G.; Levchik, S. Effect of Metal Carboxylates on the Thermal Decomposition of Cellulose. *Polym. Degrad. Stab.* **1998**, *62*, 25−31.

(29) Alongi, J.; Camino, G.; Malucelli, G. Heating Rate Effect on Char Yield from Cotton, Poly(Ethylene Terephthalate) and Blend Fabrics. *Carbohydr. Polym.* **2013**, *92*, 1327−1334.

(30) Ray, S. S. *Clay-Containing Polymer Nanocomposites, From Fundamentals to Real Applications*; Elsevier: Amsterdam, 2013; pp 263−271.

(31) Paluszkiewicza, C.; Stodolakb, E.; Hasika, M.; Blazewiczb, M. FTIR Study of Montmorillonite−Chitosan Nanocomposite Materials. *Spectrochim. Acta, Part A* **2011**, *79*, 784−788.

(32) Soares, S.; Camino, G.; Levchik, S. Comparative Study of the Thermal Decomposition of Pure Cellulose and Pulp Paper. *Polym. Degrad. Stab.* **1995**, *49*, 275−283.

(33) Frantzich, H. *A Model for Performance-Based Design of Escape Routes*, Technical report; Department of Fire Safety Engineering, Lund Institute of Technology: Lund University, Sweden, 1994.

(34) Gann, R. G. Estimating Data for Incapacitation of People by Fire Smoke. *Fire Technol.* **2004**, *40*, 201−207.

(35) Purser, D. A. In *Fire Toxicity*; Stec, A., Hull, R., Eds.; Woodhead Publishing Limited: Cambridge, U.K., 2013; Chapter 8, pp 282−342.

(36) Dumanl, A. G.; Windle, A. H. Carbon Fibres from Cellulosic Precursors: A Review. *J. Mater. Sci.* **2012**, *47*, 4236−4250.

(37) Hao, J.; Lewin, M.; Wilkie, C. A.; Wang, J. Additional Evidence for the Migration of Clay Upon Heating of Clay-Polypropylene

DOI: 10.1021/am509058h
ACS Appl. Mater. Interfaces 2015, 7, 5847−5856

Nanocomposites from X-ray Photoelectron Spectroscopy. *Polym. Degrad. Stab.* **2006**, *91*, 2482−2485.
(38) Tang, Y.; Lewin, M. Maleated Polypropylene OMTM Nanocomposite: Annealing, Structural Changes, Exfoliated and Migration. *Polym. Degrad. Stab.* **2007**, *92*, 53−60.

DOI: 10.1021/am509058h
ACS Appl. Mater. Interfaces 2015, 7, 5847−5856